J Physiol 587.11 (2009) pp 2499–2510

The Journal of Physiology

Network-based activity induced by 4-aminopyridine in rat dorsal horn *in vitro* is mediated by both chemical and electrical synapses

Rebecca J. Chapman, Paul F. Cilia La Corte, Aziz U. R. Asghar and Anne E. King

Institute for Membrane and Systems Biology, University of Leeds, Leeds LS2 9JT, UK

This study investigated the role of electrical and chemical synapses in sustaining 4-aminopyridine (4-AP)-evoked network activity recorded extracellularly from substantia gelatinosa (SG) of young rat spinal cord *in vitro*. Superfusion of 4-AP (50 μM) induced two types of activity, the first was observed as large amplitude field population spiking activity and the second manifested within the inter-spike interval as low amplitude rhythmic oscillations in the 4–12 Hz frequency range (mean peak of 8.0 ± 0.1 Hz). The AMPA/kainate receptor antagonist 6-cyano-7-nitroquinoxaline-2,3-dione (CNQX, 10 μM) abolished field population spiking and disrupted 4–12 Hz rhythmic oscillatory activity whereas the NMDA receptor antagonist D-AP5 (50 μM) had no significant effect on either activity component. The glycine receptor antagonist strychnine (4 μM) and the $GABA_A$ receptor antagonist bicuculline (10 μM) diminished and abolished, respectively, field population spiking and both antagonists reduced the power of 4–12 Hz oscillations. The non-specific gap junction blockers carbenoxolone (100 μM) and octanol (1 mM) attenuated both types of 4-AP-induced activity. By comparison, the neuronal-specific gap junction uncouplers quinine (250 μM) and mefloquine (500 nM) both disrupted 4–12 Hz oscillations but only quinine reduced the frequency of field population spiking. These data demonstrate the existence of 4-AP-sensitive neuronal networks within SG that can generate rhythmic activity, are differentially modulated by excitatory and inhibitory ionotropic neurotransmission and are at least partly reliant on neuronal and/or glial-mediated electrical connectivity. The physiological significance of these putative intrinsic SG networks and the implications in the context of processing of nociceptive inputs are discussed.

(Resubmitted 4 March 2009; accepted after revision 3 April 2009; first published online 9 April 2009)

Corresponding author A. E. King: Institute for Membrane and Systems Biology, University of Leeds, Leeds, LS2 9JT, UK. Email: a.e.king@leeds.ac.uk

Abbreviations: AMPA, α-amino-3-hydroxyl-5-methyl-4-isoxazole propionate; D-AP5, D-amino-phosphonovalerate; 4-AP, 4-aminopyridine; aCSF, artificial cerebrospinal fluid; CNS, central nervous system; CPG, central pattern generator; Cx, connexin; CNQX, 6-cyano-7-nitroquinoxaline-2,3-dione; DH, dorsal horn; EEG, electroencephalogram; GABA, γ-aminobutyric acid; NMDA, *N*-methyl-D-aspartate; SG, substantia gelatinosa; VH, ventral horn.

In rodent spinal cord, network-based rhythmic activity has been characterized mainly in the context of ventral horn (VH) locomotor central pattern generation (CPG) (Kiehn, 2006) but largely ignored in sensory dorsal horn (DH). However, in the rat DH *in vivo*, spontaneous activity recorded from multi-receptive or nociceptive neurones displayed rhythmicity with two dominant frequencies (0.5–2 Hz and 6–13 Hz) that was modulated by sensory stimuli (Sandkuhler & Eblen-Zajjur, 1994; Eblen-Zajjur & Sandkuhler, 1997) and persisted after spinalization, thus implying the existence of spatially distributed DH networks capable of supporting correlated output (Sandkuhler & Eblen-Zajjur, 1994; Sandkuhler *et al.* 1995). These *in vivo* data are supported by *in vitro* data describing rhythmic activity in the 4–12 Hz frequency range induced by elevated extracellular potassium (K^+) recorded from isolated quadrants of the neonatal rat DH (Asghar *et al.* 2005). In the brain, synchronous neuronal activity may support features of sensory processing or cognition (Varela *et al.* 2001) and such phenomena may be relevant to sensory spinal dorsal horn.

The K^+ channel blocker 4-aminopyridine (4-AP) elicits oscillatory activity in many regions of the central nervous system (CNS) and has been used as a model to advance the understanding of the organization of neuronal networks.

R. J. Chapman and P. F. Cilia La Corte contributed equally to this work.

DOI: 10.1113/jphysiol.2009.171777

In the presence of 4-AP, synchronous oscillations emerge in ventral roots of the isolated rat neonatal spinal cord and fictive locomotor patterns that reflect the output of a networked CPG are enhanced (Taccola & Nistri, 2004; Taccola & Nistri, 2005). Abolition of 4-AP-induced physiological effects by horizontal sectioning of the spinal cord suggested functional coupling of DH and VH networks, with the DH providing the main oscillatory drive (Taccola & Nistri, 2005). In decerebrate spinalized cats, 4-AP induced a sustained antidromic rhythmic discharge (2.5–8.5 Hz) which was synchronous among adjacent dorsal roots but the site of origin was unknown (Dubuc & Rossignol, 1989). 4-AP-induced spiking behaviour, which was dependent on excitatory and inhibitory neurotransmission and was most pronounced in superficial laminae, has been described for *in vitro* neonatal rat DH (Ruscheweyh & Sandkuhler, 2003). Synchronous activity, observed in spinal cord slices as oscillatory calcium waves (Ruscheweyh & Sandkuhler, 2005) are manifest in neonatal rat DH but not VH after 4-AP.

In this study, we used an *in vitro* neonatal rat lumbar spinal cord preparation to characterize patterns of 4-AP-induced activity within a specific DH lamina, namely the SG (lamina II), a region strongly linked to nociceptive processing and pain. In particular, we evaluated the relative contributions of $GABA_A$- and glycine-mediated inhibition and glutamatergic excitation via AMPA/kainate or NMDA receptors since many forms of neuronal synchrony in brain (Whittington *et al.* 2000; Flint & Connors, 1996) and spinal cord (Clarac *et al.* 2004) are reliant on ionotropic chemical synapses. Electrical synapses operate via gap junctions structurally composed of hemi-channels containing connexin (Cx) proteins that are differentially expressed in neurones and glia (Nagy *et al.* 2004). Substantive data have implicated electrical synapses in CNS network-based rhythmogenesis (Kiehn & Tresch, 2002; Sohl *et al.* 2005). Given the known contribution of electrical synapses to the synchronization of 4-AP-induced network behaviour in cortical regions (Maier *et al.* 2002), we have determined whether a role for gap junctions exists in 4-AP-induced activity recorded from SG. Some of these data have been published in an abstract (Chapman *et al.* 2007).

Methods

Spinal cord slices

All animal procedures were reviewed and approved by the University of Leeds Ethical Review Committee and performed under licence strictly in accordance with current UK legislation as defined in the Animals (Scientific Procedures) Act 1986. Female Wistar rats ($n = 37$) aged 12–16 days were terminally anaesthetized with urethane (2 g kg^{-1}, I.P.) and a dorsal laminectomy performed. The spinal cord was removed and submerged in ice-cold artificial cerebro-spinal fluid (aCSF) containing sucrose (126 mM), substituted for NaCl, to improve cell viability during slicing. Normal aCSF contained (in mM): 126 NaCl, 2.5 KCl, 1.4 NaH_2PO_4, 1.2 $MgCl_2$, 2.4 $CaCl_2$, 25 $NaHCO_3$. The lumbar region of the spinal cord was isolated, stripped of the dura and pia, and embedded in 3% agar (BDH Chemicals Ltd, Poole, UK). Transverse slices (300 μm) were cut from L3–L6 using a vibrotome (Leica VT1000S, Leica Microsystems, Nussloch GmbH, Germany). In some experiments, isolated quadrants that included laminae I–VI were prepared from intact slices by sectioning in both the horizontal and sagittal planes. DH quadrants show good viability comparable to intact transverse slices whereas more reduced preparations of a specific lamina are poorly viable. Slices were transferred to a holding chamber where they were submerged in oxygenated aCSF and maintained at 35°C for at least 1 h prior to use. Spinal cord slices were transferred to a custom built Perspex recording chamber that maintained slices in an interface between warm humidified carbogen (95% O_2–5% CO_2) and aCSF that bathed the surface of the preparation at an average flow rate of 1–1.5 ml min^{-1} (32°C).

Electrophysiology

Extracellular field recordings were made using borosilicate glass microelectrodes (2–4 MΩ) filled with normal aCSF and placed at a depth of 5–10 μm into the SG which appears under a light microscope as a translucent band within the superficial DH. Voltage waveforms were recorded and amplified (×10) by an Axoclamp 2A system (Molecular Devices, CA, USA) with further amplification (×1000) provided by a Neurolog NL106 module (Digitimer, Welwyn Garden City, UK). Voltage signals were initially filtered using a low pass band filter set at 120 Hz (Neurolog NL125, Digitimer, UK). The voltage signals in all the pharmacological experiments were filtered using a low pass band filter setting of 40 Hz (Neurolog NL125, Digitimer).

Voltage waveforms were digitized at 5 kHz and captured for further analysis on Spike 2 software (Cambridge Electronic Design, Cambridge, UK). Power spectra were generated using 1 s epochs and the amplitude of the peak frequency measured to give the power of the oscillation. Power amplitude (measured as maximum peak height in spectra) and area values (calculated as the 'area under the curve' for two cursors set at 4 and 12 Hz in spectra) were derived from an average of five consecutive 1 s epochs recorded within the inter-spike interval of large amplitude field population spiking activity. The sampling rate was 5 kHz, which divided by the 8192 points in the fast Fourier transform, to provide an overall resolution of 0.6 Hz. Spike interval histograms for individual experiments were calculated from the number of events that occurred above

one-third of the average spike height over 30 s, during field population spiking activity. Data were pooled for quantitative and statistical analyses of data sets of specific drugs tested. All data sets were tested for normality before continuing with a *t* test. For comparison of multiple data sets, one-way ANOVA and Scheffé's *post hoc* test were utilized (SPSS 12.0 for Windows, SPSS Inc, Chicago, IL, USA). Statistical analysis of power amplitude, power area and frequency were performed using a Student's *t* test for paired or unpaired data using raw data values. Data values are expressed as means ± standard error of the mean (S.E.M.). Values of $P < 0.05$ were considered statistically significant. All of the stated *n* values refer to the number of spinal slices used per experiment and taken from different animal preparations.

Drugs

Drugs were dissolved in aCSF and bath applied via separate gravity-fed inlets. 4-AP (Sigma-Aldrich, UK) was tested across the concentration range 12.5–100 μM with 50 μM selected for the pharmacological studies since this concentration produced stable long-lasting DH activity and has been used previously to elicit maintained oscillatory behaviour in neonatal spinal cord slices (Taccola & Nistri, 2005). Bicuculline methiodide (a $GABA_A$ receptor antagonist, concentration used 10 μM), strychnine (a glycine receptor antagonist, 4 μM), D(−)-2-amino-5-phosphonopentanoic acid (D-AP5, an NMDA receptor antagonist, 50 μM), and 6-cyano-7-nitroquinoxaline-2,3-dione (CNQX, an AMPA/kainate receptor antagonist, 10 μM) were all purchased from Tocris Cookon (Bristol, UK). The non-specific gap junction uncouplers octanol (1 mM) and carbenoxolone (100 μM) (Rozental *et al.* 2001) and the anti-malarial drug quinine (250 μM), which targets more selectively neuronal gap junctions that express Cx36 and Cx50 (Srinivas *et al.* 2001), were purchased from Sigma (UK). Mefloquine (500 nM), another more potent selective neuronal gap junction uncoupler (Cruikshank *et al.* 2004), was obtained from MP Biomedicals Europe, Illkirch, France. The concentrations of all gap junction uncouplers used here are based on previously published effective doses. In protocols for testing the drug actions, 4-AP was perfused initially for a period of 30–45 min in order to establish stable baseline activity against which drugs were tested. Full or partial reversibility of all drug actions was achieved after prolonged drug washout.

Results

4-AP-induced activity in SG *in vitro*

In slices bathed in control aCSF ongoing low level spontaneous neuronal activity was recorded in SG, as monitored by extracellular field recordings (Fig. 1*A*). This spontaneous activity was mainly asynchronous although brief transient episodes of weakly rhythmic activity were observed (Fig. 1*B* and *C*). Following superfusion of 4-AP (50 μM), two types of activity emerged: large amplitude field population spikes (Fig. 1*Aa*) and within the inter-spike interval low amplitude voltage oscillations (Fig. 1*Ab*). Field population spiking activity (Fig. 1*A*) with an amplitude range of 50–300 μV and inter-spike interval range of 0.3–3.5 s (Fig. 1*D*) manifested within 10–15 min post-4-AP application. Low amplitude voltage oscillations (< 20 μV) arising from inter-spike baseline activity (Fig. 1*A*) occurred after more prolonged exposure to 4-AP (> 30 min). This activity possessed a distinctive rhythmic characteristic, oscillating within the 4–12 Hz frequency band (Fig. 1*B*) with a dominant mean peak frequency of 8.0 ± 0.1 Hz ($n = 37$) and lasted for either part or the whole of the inter-spike interval. The peak power amplitude and the power area of the 4–12 Hz rhythmic activity was significantly different from baseline activity recorded in control aCSF ($P < 0.05$, $n = 37$; Fig. 1*C*). Quantified data derived from spectra ($n = 6$), indicated a concentration-related effect of increasing 4-AP concentrations (12.5, 25, 50 and 100 μM) on power amplitude (expressed as 10^{-6} V^2: 1.65 ± 0.34, 3.08 ± 0.58, 5.19 ± 1.95, 6.78 ± 2.3, respectively) and power area (6.6 ± 1.57, 9.7 ± 1.99, 15.96 ± 5.5, 20.49 ± 7.34, respectively) whilst the frequency was consistently within the 4–12 Hz range. The incidence of large amplitude field population spiking also increased over the same concentration range (0.32 ± 0.06, 0.53 ± 0.08, 0.75 ± 0.12, 0.78 ± 0.13 Hz; $n = 6$). Typically, stable 4-AP-evoked activity could be recorded for a period of up to 3 h and activity levels returned to baseline upon wash to normal aCSF. Data derived for frequency of field population spiking activity and power amplitude or power area of 4–12 Hz oscillations were not significantly different across tested time points of 30, 60, 120 and 180 min (50 μM 4-AP, $n = 3$, $P > 0.05$). In order to determine whether 4-AP-induced activity could be supported solely by intrinsic ipsilateral DH circuitry, recordings were made within the SG of DH quadrants that were anatomically isolated from VH and contralateral DH by combined sagittal and horizontal sectioning of the spinal cord slice (Fig. 2*A*). As was observed for intact spinal cord slices, 4-AP (50 μM) induced large amplitude field population spikes (amplitudes ranging from 30–300 μV; Fig. 2*B*) and low amplitude voltage oscillations within the inter-spike interval (Fig. 2*B*) that displayed rhythmicity in the 4–12 Hz frequency range. The peak power amplitude and the power area values of the 4–12 Hz rhythmic oscillatory component were significantly increased compared to control activity recorded in aCSF ($P < 0.05$, $n = 18$; Fig. 2*Ca* and *b*).

Contributions of excitatory and inhibitory neurotransmission to 4-AP-induced activity in SG

The AMPA/kainate receptor antagonist CNQX (10 μM) abolished large amplitude field population spiking activity (Fig. 3*Aa*) induced by 4-AP (50 μM, 30 min) and disrupted low amplitude 4–12 Hz rhythmic oscillatory activity, as evidenced by the significantly attenuated peak power amplitude and power area values ($P < 0.05$, $n = 7$; Fig. 3*Aa–c*). CNQX caused a significant and reversible $68 \pm 7\%$ attenuation in the peak power amplitude and a significant $49 \pm 9\%$ reversible reduction in the peak power area of the 4–12 Hz inter-spike rhythmic oscillation (Figs 3*Ac* and 4*A*). In the presence of CNQX, there was a small but significant enhancement of peak frequency from 7.8 ± 0.1 Hz to 8.5 ± 0.1 Hz ($P < 0.05$, $n = 7$). In contrast, the selective NMDA receptor antagonist D-AP5 (50 μM, $n = 4$) had no significant effect on the incidence of large amplitude field population spikes induced by 4-AP (mean value of 0.96 ± 0.1 Hz in aCSF *versus* 0.80 ± 0.1 Hz, $P > 0.05$) although their overall amplitude was reduced (Fig. 3*Ba*). Similarly, D-AP5 had no substantive effect on the 4–12 Hz low amplitude inter-spike voltage oscillations ($P > 0.05$, $n = 5$), as reflected in mean values calculated for peak power amplitude and area of the 4–12 Hz rhythm pre- and post D-AP5 (Figs 3*Bb* and *c* and 4*A*). Mean reductions of $12 \pm 10\%$ and $4 \pm 9\%$ for peak power area and amplitude, respectively, were produced by D-AP5, values that were not statistically significant ($P > 0.05$, $n = 4$). D-AP5 had no significant effect on the peak frequency of oscillations (8.3 ± 0.2 Hz in control aCSF compared to 8.0 ± 0.2 Hz after D-AP5; $P > 0.05$, $n = 4$). The effects of the glutamate ionotropic receptor antagonists CNQX and D-AP5 on the two types of 4-AP-induced activity in SG are summarized in Table 1.

Application of the $GABA_A$ receptor antagonist bicuculline (10 μM, $n = 7$) abolished large amplitude field population spiking activity (Fig. 5*Aa*) whilst the glycine receptor antagonist strychnine (4 μM, $n = 6$) reversibly and significantly reduced (from 0.7 ± 0.1 Hz to

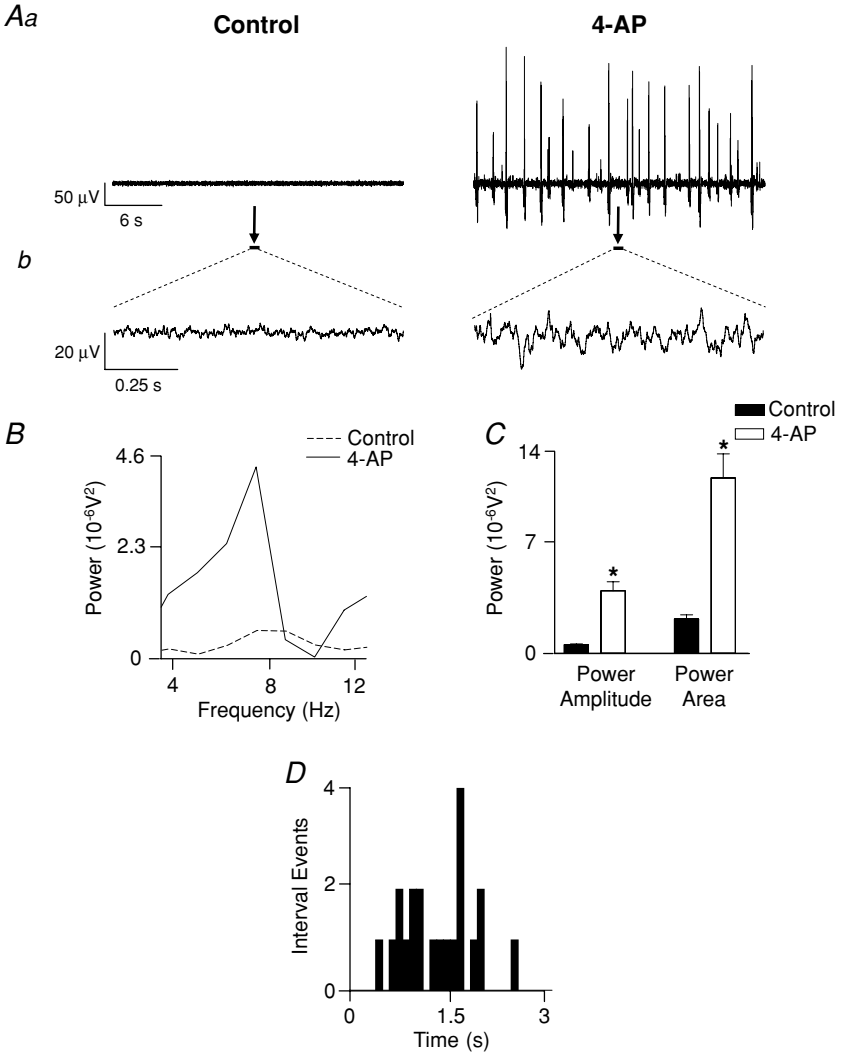

Figure 1. 4-AP evokes two profiles of activity in SG of the rat spinal cord *in vitro*
A, 4-AP (50 μM) induced large amplitude field population spiking activity (*Aa*, right trace) and low amplitude rhythmic oscillations within the baseline of the field population spiking inter-spike interval (*Ab*, sample expanded 1 s epochs indicated by arrows and black bars in *Aa*). *B*, power spectra of low amplitude rhythmic oscillations reveal a dominant frequency within the 4–12 Hz frequency band after 4-AP (dashed line, control; continuous line, 4-AP). *C*, quantified data ($n = 37$) reveal a significant increase in spectra power amplitude and area (*$P < 0.05$) after 4-AP (control, black bar; 4-AP, white bar). *D*, analysis of large amplitude field population activity (recorded from same preparation as *Aa*) revealed a range of inter-spike intervals and no regularity in spike occurrence.

0.3 ± 0.03 Hz, $P < 0.05$) field population spiking activity (Fig. 5*Ba*). Bicuculline and strychnine also significantly disrupted low amplitude rhythmic voltage oscillations (Fig. 5*Ab* and *Bb*) and attenuated the measured peak power amplitude and power area values (Fig. 5*Ac* and *Bc*). Spectral analysis of this inter-spike 4–12 Hz rhythmic component revealed significant reductions of $63 \pm 8\%$ in peak power area and $42 \pm 14\%$ in peak power area by bicuculline ($P < 0.05$, $n = 7$; Fig. 4*A*). Strychnine significantly attenuated the peak power amplitude by $63 \pm 6\%$ and the power area by $56 \pm 10\%$ ($P < 0.05$, $n = 6$; Fig. 4*A*). However, neither bicuculline nor strychnine significantly affected the peak frequency of the inter-spike 4–12 Hz rhythmic component (7.8 ± 0.3 Hz in 4-AP compared to 7.7 ± 0.4 Hz, $n = 7$, in bicuculline and 8.3 ± 0.2 Hz in 4-AP compared to 8.25 ± 0.3 Hz, $n = 6$, in strychnine; both $P > 0.05$). The effects of the two inhibitory receptor antagonists bicuculline and strychnine on 4-AP-induced activity in SG are summarized in Table 1.

The role of gap junctions in SG 4-AP-mediated activity

The non-specific gap junction uncouplers carbenoxolone (100 μM, $n = 7$) and octanol (1 mM, $n = 10$) significantly attenuated 4-AP-induced activity in SG. Carbenoxolone reduced field population spiking activity (from 0.8 ± 0.3 Hz in 4-AP to 0.2 ± 0.2 Hz, $n = 7$) whilst octanol abolished it (Fig. 6*Aa* and *Ba*). There was also a strong degradation of the inter-spike 4–12 Hz rhythmic oscillatory component (Fig. 6*Ab* and *Bb*), as indicated by reductions in both the peak power amplitude and area (Fig. 6*Ac* and *Bc*). Quantified data derived from spectra revealed a $46 \pm 8\%$ decrease in power amplitude and a $40 \pm 10\%$ decrease in power area ($P < 0.05$, $n = 7$; Figs 6*Ac* and 4*B*) after carbenoxolone. The effects of carbenoxolone were only partially reversed following prolonged washout. Octanol induced a reversible $62 \pm 5\%$ reduction in power amplitude ($P < 0.05$, $n = 10$; Fig. 4*B*) and a $60 \pm 6\%$ reduction in power area ($P < 0.05$, $n = 10$; Fig. 4*B*). Neither of the gap junction uncouplers significantly affected the dominant 4–12 Hz frequency of this component (7.29 ± 0.3 Hz in 4-AP compared to 6.91 ± 0.31 Hz in carbenoxolone, $P > 0.05$, $n = 7$; 7.71 ± 0.17 Hz in 4-AP compared to 7.14 ± 0.16 Hz in octanol, $n = 10$).

The neuronal-specific gap junction uncoupler quinine (250 μM, $n = 9$) induced a significant reversible reduction in peak power amplitude and power area ($52 \pm 7\%$ and $52 \pm 6\%$ reductions respectively, $P < 0.05$, Figs 7*Ab*, *Ac* and 4*B*) of the low amplitude inter-spike 4–12 Hz rhythm. Similarly, mefloquine (500 nM, $n = 9$) induced a profound but reversible attenuation of peak power amplitude ($40 \pm 7\%$ decrease) and power area ($37 \pm 8\%$ decrease, $P < 0.05$, $n = 9$; Fig. 7*Bb*, *Bc* and 4*B*). Additionally, quinine significantly reduced field population spiking activity, from 0.6 ± 0.1 Hz in 4-AP to 0.35 ± 0.1 Hz in quinine ($P < 0.05$, $n = 9$) whilst mefloquine had no effect ($P > 0.05$, $n = 9$; Fig. 7*Aa* and

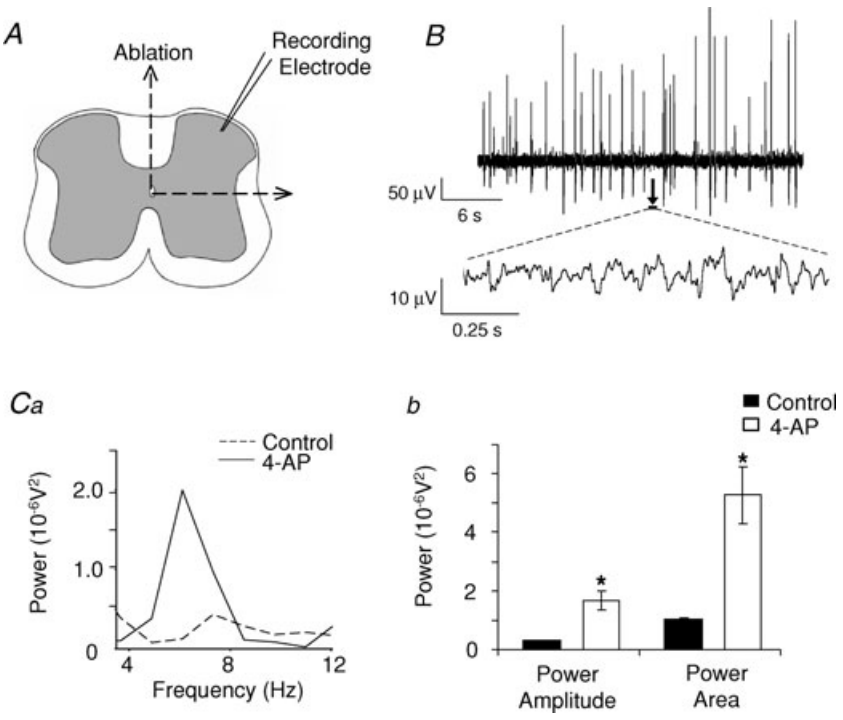

Figure 2. 4-AP evokes two profiles of activity in SG of isolated DH quadrants *in vitro*
A, to isolate the DH from contralateral DH and ipsi- or contralateral ventral regions, intact spinal cord slices were lesioned vertically through the midline and horizontally just below lamina V/VI. *B*, 4-AP (50 μM) induced two profiles of activity similar to that observed in intact slices, namely large amplitude field population spiking activity (*B*, upper trace) and low amplitude rhythmic oscillations within the inter-spike interval (*B*, lower trace, sample expanded 1 s epochs indicated by arrow and black bar). *Ca*, power spectra of the low amplitude rhythmic oscillations reveal a peak 4–12 Hz frequency band with increased power amplitude and area (*Cb*) during 4-AP application (dashed line, control; continuous line, 4-AP).

Ba). Neither drug affected peak frequency of the 4–12 Hz component (control value of 7.11 ± 0.18 Hz *versus* 7.01 ± 0.13 Hz after quinine, $P > 0.05$, control value of 7.19 ± 0.21 Hz *versus* 6.93 ± 0.13 Hz after mefloquine). The effects of the gap junction uncouplers on the two types of 4-AP-induced activity in SG are summarized in Table 1.

Discussion

4-AP induces a novel form of 4–12 Hz rhythmic behaviour in SG

In this study, 4-AP generated two types of activity localized to lumbar SG *in vitro*. The first activity profile to emerge took the form of large amplitude field population spikes with properties similar to those described in rat superficial DH *in vitro* (Ruscheweyh & Sandkuhler, 2003) or in VH locomotor circuitry *in vitro* (Taccola & Nistri, 2005). A second hitherto unreported form of low amplitude 4–12 Hz oscillatory activity subsequently emerged from within the baseline of the inter-spike interval of the extracellular field population spiking. In this respect, it resembles rhythmic behaviour that manifests in SG *in vitro* after localized elevation of K^+ and is attributed to neuronal networks within DH (Asghar *et al.* 2005). An *in vivo* correlate of rhythmic behaviour (0.5–13 Hz) has been extracted from background discharges of DH neurones (Sandkuhler & Eblen-Zajjur, 1994). These *in vivo* and *in vitro* data support the concept of intrinsic DH neuronal ensembles that can fire synchronously to generate a temporally defined output. The finding here that both types of 4-AP activity could be recorded from SG of isolated DH quadrants further indicated the sufficiency of DH circuitry and the localization of 4-AP-sensitive targets to this area.

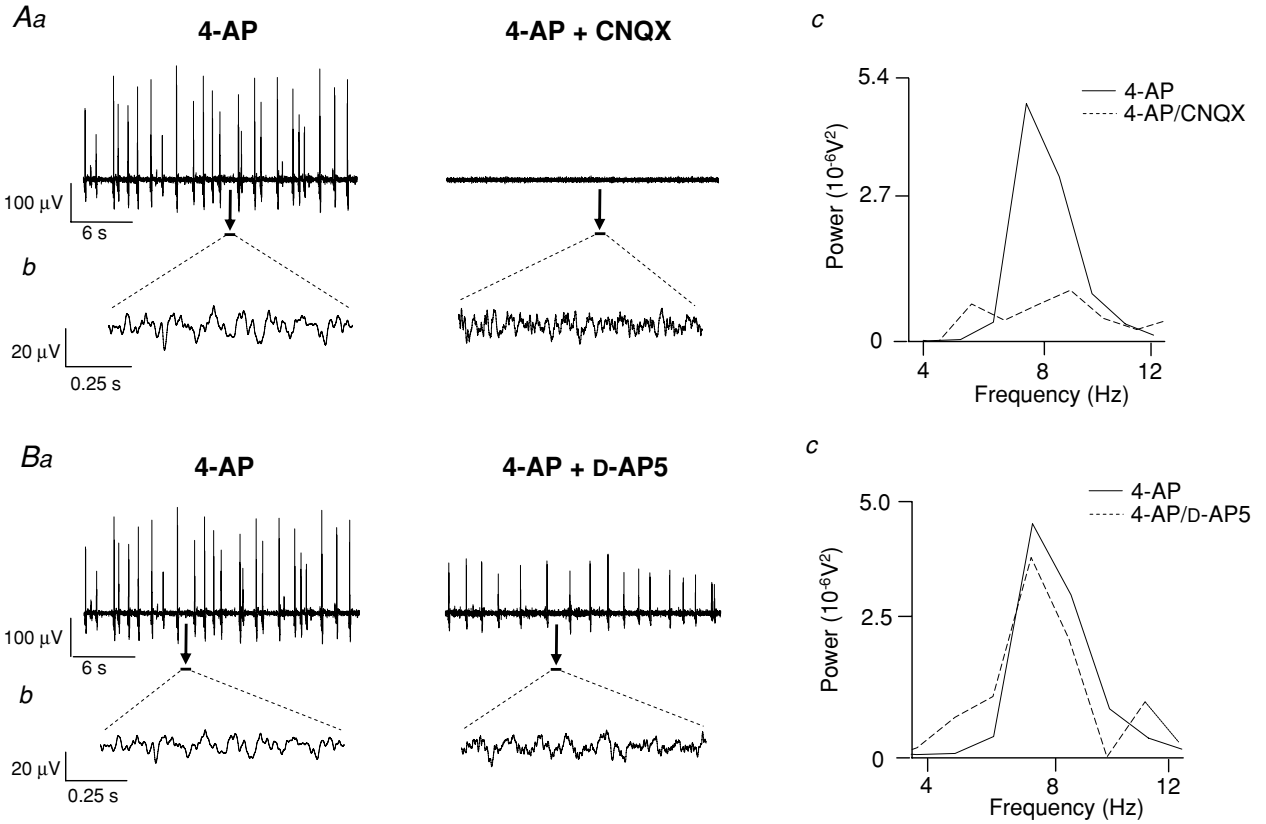

Figure 3. The glutamate receptor antagonist CNQX but not D-AP5 attenuates 4-AP-induced activity in SG

Aa, large amplitude field potential activity induced by 4-AP (50 μM) is abolished by CNQX (10 μM). *Ab*, 4–12 Hz rhythmic oscillatory activity recorded within the inter-spike interval (sample expanded 1 s epochs denoted by black bars and arrows in *Aa*) is disrupted by CNQX. *Ac*, power spectra analysis revealed a lack of rhythmicity in this component after CNQX (4-AP, continuous line; CNQX, dashed line). *Ba*, The incidence of large amplitude field potential spikes is not significantly affected by D-AP5 (50 μM) although the amplitude is reduced. *Bb*, examples of 4–12 Hz rhythmic oscillatory activity (expanded 1 s epoch denoted by black bars in *Ba*) in control (4-AP, left trace) and after D-AP5 (right trace). *Bc*, power spectra of activity reveal no significant change in peak frequency, power area or amplitude after D-AP5 (4-AP, continuous line; D-AP5, dashed line; $n = 4$).

Self-contained rhythmogenic activity in DH quadrants has been demonstrated using voltage imaging (Demir *et al.* 2002) and dorsal root recordings (Taccola & Nistri, 2005) in developing rats. Ca^{2+} transients and correlated neuronal firing induced by 4-AP in rat DH *in vitro* revealed initiation within medial superficial DH, with propagation to other DH regions (Ruscheweyh & Sandkuhler, 2005). As a K^+ channel blocker with selectivity towards A-currents, 4-AP has pre- and postsynaptic actions. Presynaptic terminal action potential broadening increases transmitter release whilst postsynaptic I_A inhibition enhances neuronal excitability. Since I_A is generated by Kv subunits especially Kv4, one may speculate on an involvement of Kv4.2-expressing neurones in superficial DH (Hu *et al.* 2006) in rhythmogenesis. Interestingly, 4-AP-sensitive K^+ channels contribute to the anti-nociceptive actions of $GABA_B$ agonists (Ocana *et al.* 2004).

The difference in the time to onset of the two types of 4-AP-induced activity is intriguing but difficult to interpret. In considering the two forms of 4-AP-induced activity, population field spiking and 4–12 Hz oscillations, it is possible that a single network underlies both forms or alternatively distinct mechanisms may underpin each. The finding that drugs such as CNQX, bicuculline or octanol abolished field population spiking whilst 4–12 Hz oscillations remained active (albeit with reduced power) could be interpreted as indicating separate mechanisms. Similarly, mefloquine compromised 4–12 Hz oscillations without affecting field population spikes. Further studies are required to determine the exact nature of the relationship, if any, between the two types of 4-AP-induced activity. Another unresolved issue is the extent to which neurones with pacemaker-like intrinsic membrane properties may contribute to the 4–12 Hz oscillatory output. Certainly in VH CPG circuitry there is evidence for classes of interneurones that possess rhythmogenic pacemaker-like properties (Clarac *et al.* 2004; Kiehn, 2006). Abolition by TTX of all 4-AP induced network spiking activity (Taccola & Nistri, 2005) inferred a strong reliance on synapses rather than pacemaker neurones. However, in the context of 4-AP-induced oscillatory activity in SG this question remains to be answered.

Table 1. Comparison of effects of ionotropic receptor antagonists and gap junction uncouplers on 4-AP-induced activity in SG

Drug (conc., mM)	Field population spiking	4–12 Hz oscillation
Ionotropic receptor antagonists		
CNQX (10 μM)	↓↓↓	↓
D-AP5 (50 μM)	↔	↔
Bicuculline (10 μM)	↓↓↓	↓
Strychnine (4 μM)	↓	↓
Gap junction uncouplers		
Carbenoxolone (100 μM)	↓	↓
Octanol (1 mM)	↓↓↓	↓
Quinine (250 μM)	↓	↓
Mefloquine (500 nM)	↔	↓

↔, no effect; ↓, decreased but not abolished; ↓ ↓ ↓, abolished.

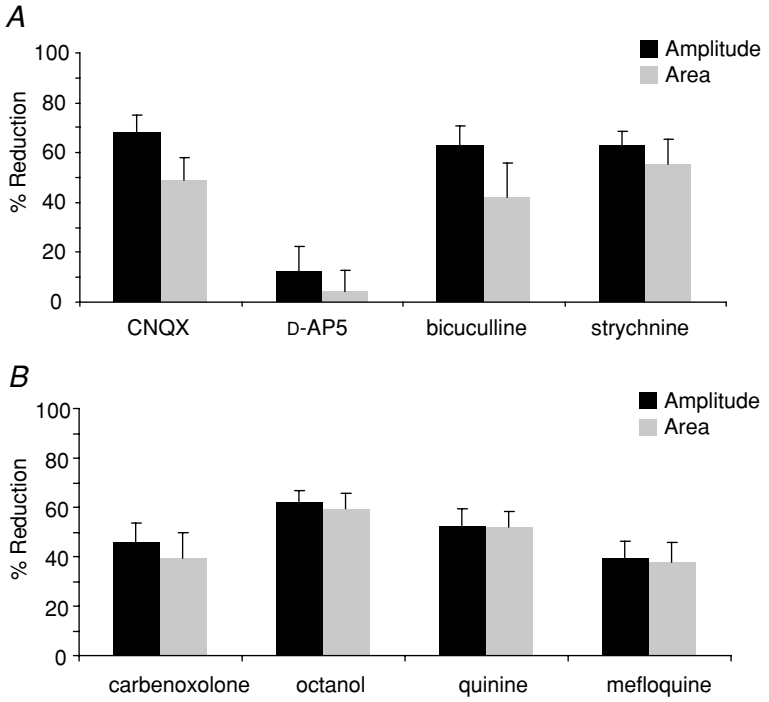

Figure 4. Quantified data for drug actions on 4–12 Hz rhythmic oscillatory activity in SG
A, CNQX (10 μM, $n = 7$), bicuculline (10 μM, $n = 7$) and strychnine (4 μM, $n = 6$) all significantly reduced power amplitudes and power areas of 4-AP (50 μM) induced rhythmic oscillatory activity whereas D-AP5 (50 μM, $n = 4$) had no effect. *B*, carbenoxolone (100 μM, $n = 7$), octanol (1 mM, $n = 10$), quinine (250 μM, $n = 9$) and mefloquine (500 nM, $n = 9$) significantly reduced power amplitudes and power areas of spectra derived from 4–12 Hz rhythmic oscillatory activity. All data for drug effects are expressed as percentage reductions against values obtained in 4-AP alone.

4-AP-induced activity is supported by chemical neurotransmission

CNQX abolished 4-AP-induced large amplitude field population spiking activity and disrupted but did not abolish low amplitude 4–12 Hz rhythmic activity in SG (Table 1) suggesting that AMPA/kainate receptor-mediated synaptic processes differentially contribute to the two types of 4-AP-induced network activity, the former being more reliant on intact AMPA/kainate receptor-mediated synaptic transmission. In contrast, D-AP5 had no significant effect on either type of activity (Table 1), inferring a minimal role for NMDA receptors. These data corroborate the requirement of AMPA/kainate receptor-mediated fast excitation for the manifestation of 4-AP-induced epileptiform spiking activity in superficial DH *in vitro* (Ruscheweyh & Sandkuhler, 2003). This is consistent with the fact that within SG, glutamate acts predominately via non-NMDA-mediated synapses (Yoshimura & Jessell, 1990). NMDA or AMPA/kainate receptor antagonists disrupt locomotor-like patterns in isolated neonatal rat spinal cord (Bracci *et al.* 1998). The lack of D-AP5 effects described here for 4-AP-induced activity in SG indicates a key difference between this DH network and VH CPG networks and suggests that 4-AP-sensitive DH networks operate independently from VH CPGs. Topographical analysis of 4-AP-evoked oscillations recorded from neonatal rat spinal cord *in vitro* similarly suggested that 4-AP-sensitive networks localized to DH were functionally distinct from VH CPG networks (Taccola & Nistri, 2005).

A role for inhibitory $GABA_A$ and glycine receptors was indicated by the attenuation or abolition of field population spiking activity and a reduction of 4–12 Hz oscillatory power by either bicuculline or strychnine (Table 1). These data accord with the diminution of epileptiform-like spiking activity (Ruscheweyh & Sandkuhler, 2003) and disruption of K^+-induced oscillations (Asghar *et al.* 2005) by GABA and glycine antagonists in SG. Similarly, 4-AP-induced rhythmic discharges recorded from dorsal roots are abolished by strychnine and bicuculline (Taccola & Nistri, 2005). In contrast, VH disinhibition elicits slow synchronous burst oscillations that are linked to CPG network output (Bracci *et al.* 1996). In analogy with cortical networks, the disruptive effect of $GABA_A$ antagonism may indicate

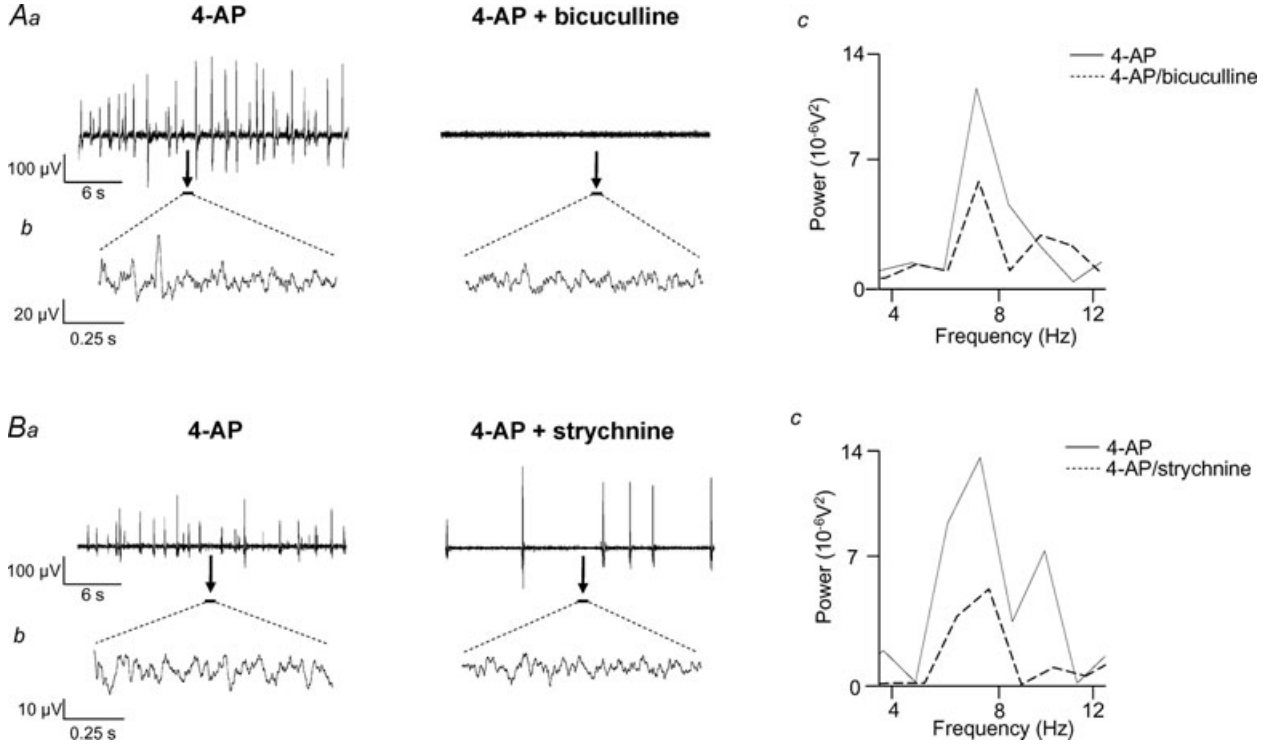

Figure 5. The inhibitory antagonists bicuculline and strychnine attenuate 4-AP-induced activity in SG
Aa and *Ba*, large amplitude field potential activity induced by 4-AP (50 μM) is abolished by bicuculline (10 μM) (*Aa*) and reduced by strychnine (4 μM) (*Ba*). *Ab* and *Bb*, examples of 4–12 Hz rhythmic oscillatory activity (expanded 1 s epochs denoted by black bars in *Aa* and *Ba*) before (left traces) and after (right traces) application of the inhibitory antagonists. *Ac* and *Bc*, power spectra reveal an attenuation of both peak power amplitude and power area in presence of bicuculline (*Ac*) or strychnine (*Bc*) (4-AP, continuous line; drug, dashed line).

reliance for rhythmicity on inhibition through coupled interneurones (Whittington *et al.* 2000). The anatomical substrates for the effects of these inhibitory antagonists are unknown but GABA-ergic interneurones (Laing *et al.* 1994), some of which contain glycine (Todd, 1996) are localized to superficial DH. $GABA_A$ (Bohlhalter *et al.* 1996) and glycine receptors (Mitchell *et al.* 1993) are abundant within laminae I–III.

4-AP induced activity in SG is supported by gap junctions

Neuronal syncitia coupled via chemical and electrical synapses may provide a mechanism for synchronization of neuronal activity in the CNS (Rozental *et al.* 2000; Sohl *et al.* 2005). Gap junctions support locomotor-like oscillations in the mouse VH (Tresch & Kiehn, 2000). Mixed chemical and electrical synapses also exist within adult rat spinal cord (Rash *et al.* 1996, 1998). Carbenoxolone and octanol disrupted both forms of 4-AP-induced activity (Table 1), inferring a contribution of gap junction connectivity to the manifestation of 4-AP-induced activity within SG *in vitro*. Interestingly, in isolated young rat spinal cord, carbenoxolone decelerated 4-AP-induced VR rhythms that originated from DH (Taccola & Nistri, 2004). Gap junctions are constituted from Cx proteins that are heterogeneously expressed in neurones or glia through the mammalian spinal cord (Rash *et al.* 2000, 2001) and are developmentally regulated (Lee *et al.* 2005). There is evidence for DH expression of Cx36 (Condorelli *et al.* 2000; Lee *et al.* 2005), Cx32 and Cx43 (Nagy & Rash, 2000; Qin *et al.* 2006), the latter especially abundant in SG (Ochalski *et al.* 1997). The poor specificity of octonal and carbenoxolone precludes any conclusion regarding the Cx subtypes responsible for their effects in SG. However, given that quinine and mefloquine target gap junctions containing Cx36 (Srinivas *et al.* 2001; Cruikshank *et al.* 2004), the finding that both drugs degraded 4-AP-induced 4–12 Hz rhythmic activity suggests Cx36 involvement. In comparing the sensitivity of the two activity profiles induced by 4-AP, the non-selective drugs had a relatively stronger effect on

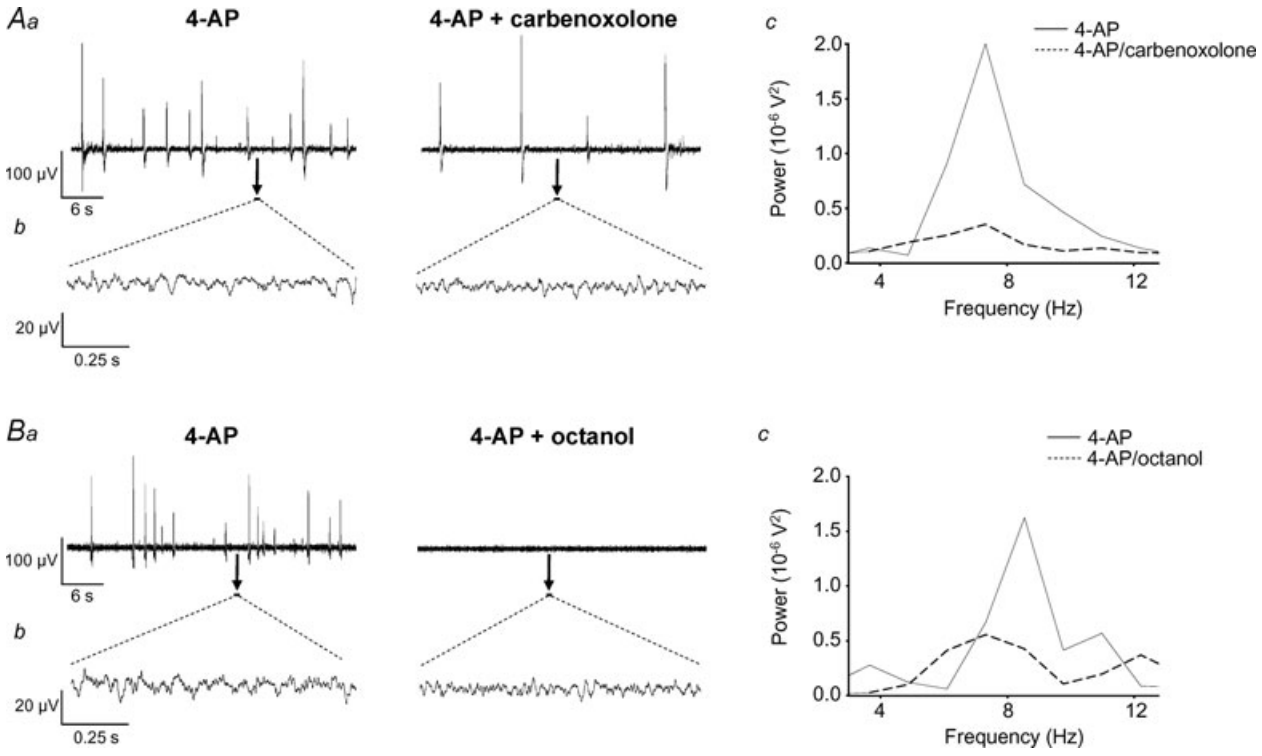

Figure 6. The non-specific gap junction uncouplers carbenoxolone and octanol disrupt 4-AP-induced activity in SG

Aa and *Ba*, large amplitude field population spikes induced by 4-AP (50 μM) were reduced by carbenoxolone (100 μM) (*Aa*) and abolished by octanol (1 mM) (*Ba*). *Ab* and *Bb*, rhythmic oscillatory activity within the inter-spike interval (expanded 1 s epochs denoted by black bars) was disrupted by either carbenoxolone (*Ab*) or octanol (*Bb*). *Ac* and *Bc*, power spectra analyses of 4–12 Hz rhythmic activity from same preparations reveal a significant attenuation of both peak power amplitude and power area (continuous line, 4-AP; dashed line, drug) in the presence of either drug.

field population spiking, which was abolished by octanol whereas mefloquine had no effect on this form of activity (Table 1). In comparison, all four drugs attenuated but did not abolish the 4–12 Hz oscillations – these variations in drug effects are likely to reflect differential expression of neuronal *versus* glial Cx proteins across the 4-AP sensitive networks.

Functional significance of rhythmicity in SG networks

The relevance of DH neuronal rhythmicity recorded from the developing rat DH *in vitro* to sensory processing in the adult remains to be established. During maturation, neural activity synchronized though gap junctions and ionotropic receptor processes undoubtedly shapes network connectivity and influences final network architecture (Roerig & Feller, 2000). However, co-ordinated spatial/temporal recruitment of defined neuronal assemblies in adult DH could provide a modality encoding mechanism or operate an 'information gate' that allows neurones to select or reject inputs based on frequency characteristics (Coghill *et al.* 1993; Sandkuhler *et al.* 1995). A corollary of this is that disruption of network coherence or inappropriate recruitment of superficial or deep DH neurones into a network that breaches normal somatotopic boundaries could contribute to aberrant sensory processing. In the context of nociceptive processing and pain, mature DH neurones *in vivo* displayed intrinsic rhythmicity that was modulated by nociceptive stimuli or inflammation (Eblen-Zajjur & Sandkuhler, 1997) and coherence between neurones in superficial and deep DH laminae was disrupted in neuropathic rats (Biella *et al.* 1997). In contrast, spinal nociceptive neurones *in vivo* after peripheral inflammation showed increased coherency (Galhardo *et al.* 2002) and similarly laminae II/III DH neurones were more prone to synchronicity following peripheral nerve injury (Schoffnegger *et al.* 2008). Gap junction coupled networks are implicated in the aetiology of neuropathic spreading pain sensations (Spataro *et al.*

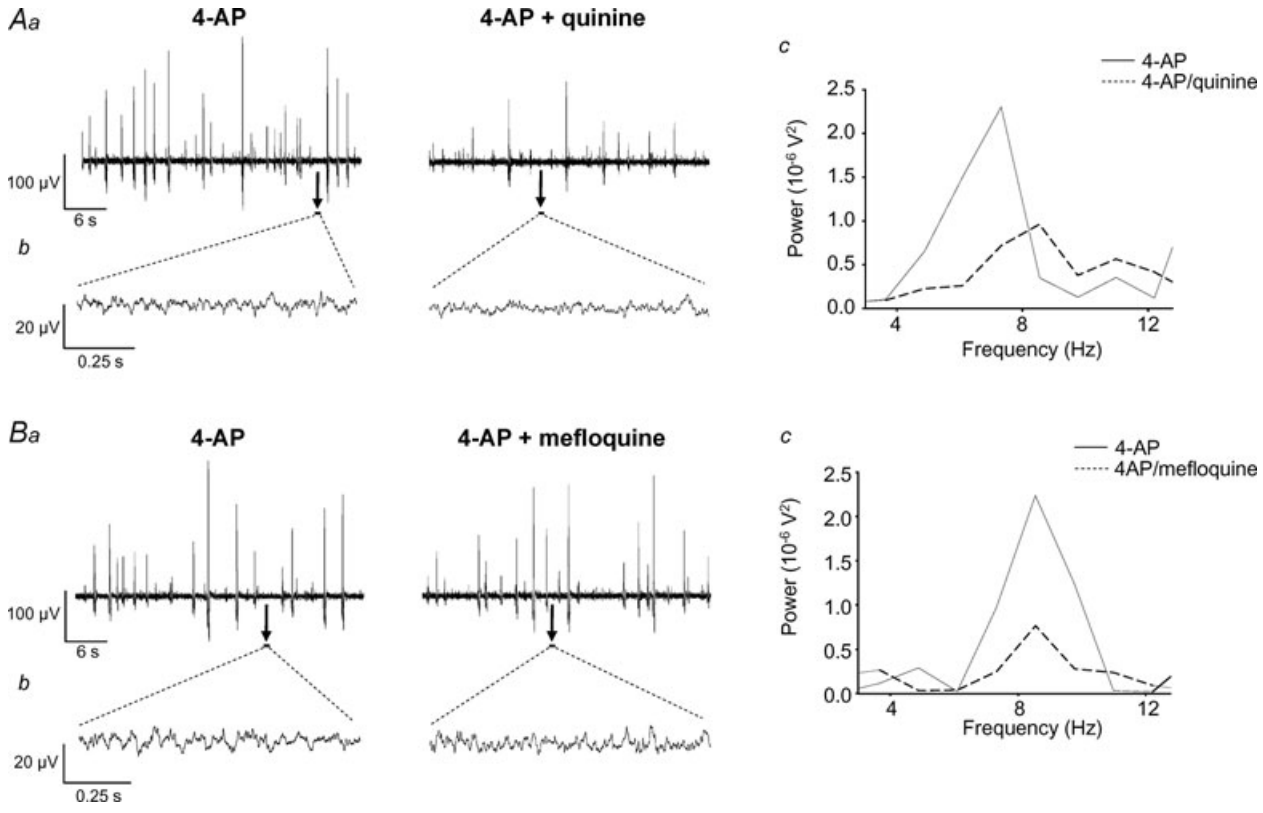

Figure 7. The neuronal specific gap junction uncouplers quinine and mefloquine disrupt 4-AP-induced activity in SG

Aa and *Ba*, large amplitude field population activity was reduced by quinine (250 μM) (*Aa*) but was less affected by mefloquine (500 nM) (*Ba*). *Ab* and *Bb*, representative examples of rhythmic oscillatory activity (expanded 1 s epochs denoted by black bars) are shown before and after either quinine (*Ab*) or mefloquine (*Bb*). *Ac* and *Bc*, spectral analysis of 4–12 Hz rhythmic component reveals a significant attenuation of peak power amplitude and area (continuous line, 4-AP; dashed line, drug) by either quinine (*Ac*) or mefloquine (*Bc*).

2004). Carbenoxolone blocks mechanical allodynia and thermal hyperalgesia induced by nerve inflammation or partial nerve injury (Spataro *et al.* 2004) and reduces formalin-induced hyperalgesia (Qin *et al.* 2006). A recent study of neurogenic pain (Sarnthein *et al.* 2006) revealed a shift to lower frequencies, notably in the 7–9 Hz band in power spectra of EEGs in human subjects. They proposed a thalamo-cortical loop oscillating at this frequency but did not investigate spinal contributions. Other human studies revealed that specific cortical areas, referred to as 'pain networks', are functionally connected during attention to painful stimuli, as evidenced by increased synchrony between structures receiving nociceptor inputs (Ohara *et al.* 2006).

In summary, these data reveal the existence within SG of neuronal networks, co-reliant upon chemical and electrical transmission, that are capable of generating a synchronized patterned output. Further studies are required to validate a physiological function for such networks and to probe their role in DH sensory processing.

References

Asghar AU, Cilia La Corte PF, LeBeau FE, Al Dawoud M, Reilly SC, Buhl EH, Whittington MA & King AE (2005). Oscillatory activity within rat substantia gelatinosa in vitro: a role for chemical and electrical neurotransmission. *J Physiol* **562**, 183–198.

Biella G, Riva L & Sotgiu ML (1997). Interaction between neurons in different laminae of the dorsal horn of the spinal cord. A correlation study in normal and neuropathic rats. *Eur J Neurosci* **9**, 1017–1025.

Bohlhalter S, Weinmann O, Mohler H & Fritschy JM (1996). Laminar compartmentalization of $GABA_A$-receptor subtypes in the spinal cord: an immunohistochemical study. *J Neurosci* **16**, 283–297.

Bracci E, Ballerini L & Nistri A (1996). Spontaneous rhythmic bursts induced by pharmacological block of inhibition in lumbar motoneurons of the neonatal rat spinal cord. *J Neurophysiol* **75**, 640–647.

Bracci E, Beato M & Nistri A (1998). Extracellular K^+ induces locomotor-like patterns in the rat spinal cord in vitro: Comparison with NMDA or 5-HT induced activity. *J Neurophysiol* **79**, 2643–2652.

Chapman RJ, Cilia La Corte PF & King AE (2007). Network-based rhythmic activity induced by 4-aminopyridine in rat dorsal horn *in vitro*: contribution of gap junction-mediated connectivity. *BNA Abstracts* 59.02.

Clarac F, Pearlstein E, Pflieger JF & Vinay L (2004). The in vitro neonatal rat spinal cord preparation: a new insight into mammalian locomotor mechanisms. *J Comp Physiol A Neuroethol Sens Neural Behav Physiol* **190**, 343–357.

Coghill RC, Mayer DJ & Price DD (1993). The roles of spatial recruitment and discharge frequency in spinal cord coding of pain: a combined electrophysiological and imaging investigation. *Pain* **53**, 295–309.

Condorelli DF, Belluardo N, Trovato-Salinaro A & Mudo G (2000). Expression of Cx36 in mammalian neurons. *Brain Res Rev* **32**, 72–85.

Cruikshank SJ, Hopperstad M, Younger M, Connors BW, Spray DC & Srinivas M (2004). Potent block of Cx36 and Cx50 gap junction channels by mefloquine. *Proc Natl Acad Sci U S A* **101**, 12364–12369.

Demir R, Gao BX, Jackson MB & Ziskind-Conhaim L (2002). Interactions between multiple rhythm generators produce complex patterns of oscillation in the developing rat spinal cord. *J Neurophysiol* **87**, 1094–1105.

Dubuc R & Rossignol S (1989). The Effects of 4-aminopyridine on the cat spinal cord: rhythmic antidromic discharges recorded from the dorsal roots. *Brain Res* **491**, 335–348.

Eblen-Zajjur AA & Sandkuhler J (1997). Synchronicity of nociceptive and non-nociceptive adjacent neurons in the spinal dorsal horn of the rat: stimulus-induced plasticity. *Neuroscience* **76**, 39–54.

Flint AC & Connors BW (1996). Two types of network oscillations in neocortex mediated by distinct glutamate receptor subtypes and neuronal populations. *J Neurophysiol* **75**, 951–957.

Galhardo V, Apkarian AV & Lima D (2002). Peripheral inflammation increases the functional coherency of spinal responses to tactile but not nociceptive stimulation. *J Neurophysiol* **88**, 2096–2103.

Hu HJ, Carrasquillo Y, Karim F, Jung WE, Nerbonne JM, Schwarz TL & Gereau RW (2006). The kv4.2 potassium channel subunit is required for pain plasticity. *Neuron* **50**, 89–100.

Kiehn O (2006). Locomotor circuits in the mammalian spinal cord. *Annu Rev Neurosci* **29**, 279–306.

Kiehn O & Tresch MC (2002). Gap junctions and motor behavior. *Trends Neurosci* **25**, 108–115.

Laing I, Todd AJ, Heizmann CW & Schmidt HHHW (1994). Subpopulations of GABAergic neurons in laminae I-III of rat spinal dorsal horn defined by coexistence with classical transmitters, peptides, nitric oxide synthase or parvalbumin. *Neuroscience* **61**, 123–132.

Lee IH, Lindqvist E, Kiehn O, Widenfalk J & Olson L (2005). Glial and neuronal connexin expression patterns in the rat spinal cord during development and following injury. *J Comp Neurol* **489**, 1–10.

Maier N, Guldenagel M, Sohl G, Siegmund H, Willecke K & Draguhn A (2002). Reduction of high-frequency network oscillations (ripples) and pathological network discharges in hippocampal slices from connexin 36-deficient mice. *J Physiol* **541**, 521–528.

Mitchell K, Spike RC & Todd AJ (1993). An immunocytochemical study of glycine receptor and GABA in laminae I-III of rat spinal dorsal horn. *J Neurosci* **13**, 2371–2381.

Nagy JI, Dudek FE & Rash JE (2004). Update on connexins and gap junctions in neurons and glia in the mammalian nervous system. *Brain Res Rev* **47**, 191–215.

Nagy JI & Rash JE (2000). Connexins and gap junctions of astrocytes and oligodendrocytes in the CNS. *Brain Res Rev* **32**, 29–44.

Ocana M, Cendan CM, Cobos EJ, Entrena JM & Baeyens JM (2004). Potassium channels and pain: present realities and future opportunities. *Eur J Pharmacol* **500**, 203–219.

Ochalski PA, Frankenstein UN, Hertzberg EL & Nagy JI (1997). Connexin-43 in rat spinal cord: localization in astrocytes and identification of heterotypic astro-oligodendrocytic gap junctions. *Neuroscience* **76**, 931–945.

Ohara S, Crone NE, Weiss N & Lenz FA (2006). Analysis of synchrony demonstrates 'pain networks' defined by rapidly switching, task-specific, functional connectivity between pain-related cortical structures. *Pain* **123**, 244–253.

Qin M, Wang JJ, Cao R, Zhang H, Duan L, Gao B, Xiong YF, Chen LW & Rao ZR (2006). The lumbar spinal cord glial cells actively modulate subcutaneous formalin induced hyperalgesia in the rat. *Neurosci Res* **55**, 442–450.

Rash JE, Dillman RK, Bilhartz BL, Duffy HS, Whalen LR & Yasumura T (1996). Mixed synapses discovered and mapped throughout mammalian spinal cord. *Proc Natl Acad Sci U S A* **93**, 4235–4239.

Rash JE, Staines WA, Yasumura T, Patel D, Furman CS, Stelmack GL & Nagy JI (2000). Immunogold evidence that neuronal gap junctions in adult rat brain and spinal cord contain connexin-36 but not connexin-32 or connexin-43. *Proc Natl Acad Sci U S A* **97**, 7573–7578.

Rash JE, Yasumura T, Davidson KG, Furman CS, Dudek FE & Nagy JI (2001). Identification of cells expressing Cx43, Cx30, Cx26, Cx32 and Cx36 in gap junctions of rat brain and spinal cord. *Cell Commun Adhes* **8**, 315–320.

Rash JE, Yasumura T & Dudek FE (1998). Ultrastructure, histological distribution, and freeze-fracture immunocytochemistry, of gap junctions in rat brain and spinal cord. *Cell Biology Int* **22**, 731–749.

Roerig B & Feller MB (2000). Neurotransmitters and gap junctions in developing neural circuits. *Brain Res Rev* **32**, 86–114.

Rozental R, Giaume C & Spray DC (2000). Gap junctions in the nervous system. *Brain Res Rev* **32**, 11–15.

Rozental R, Srinivas M & Spray DC (2001). How to close a gap junction channel. Efficacies and potencies of uncoupling agents. *Methods Mol Biol* **154**, 447–476.

Ruscheweyh R & Sandkuhler J (2003). Epileptiform activity in rat spinal dorsal horn in vitro has common features with neuropathic pain. *Pain* **105**, 327–338.

Ruscheweyh R & Sandkuhler J (2005). Long-range oscillatory Ca^{2+} waves in rat spinal dorsal horn. *Eur J Neurosci* **22**, 1967–1976.

Sandkuhler J, Eblen-Zajjur A, Fu QG & Forster C (1995). Differential effects of spinalization on discharge patterns and discharge rates of simultaneously recorded nociceptive and non-nociceptive spinal dorsal horn neurons. *Pain* **60**, 55–65.

Sandkuhler J & Eblen-Zajjur AA (1994). Identification and characterization of rhythmic nociceptive and non-nociceptive spinal dorsal horn neurons in the rat. *Neuroscience* **61**, 991–1006.

Sarnthein J, Stern J, Aufenberg C, Rousson V & Jeanmonod D (2006). Increased EEG power and slowed dominant frequency in patients with neurogenic pain. *Brain* **129**, 55–64.

Schoffnegger D, Ruscheweyh R & Sandkuhler J (2008). Spread of excitation across modality borders in spinal dorsal horn of neuropathic rats. *Pain* **135**, 300–310.

Sohl G, Maxeiner S & Willecke K (2005). Expression and functions of neuronal gap junctions. *Nat Rev Neurosci* **6**, 191–200.

Spataro LE, Sloane EM, Milligan ED, Wieseler-Frank J, Schoeniger D, Jekich BM, Barrientos RM, Maier SF & Watkins LR (2004). Spinal gap junctions: potential involvement in pain facilitation. *J Pain* **5**, 392–405.

Srinivas M, Hopperstad MG & Spray DC (2001). Quinine blocks specific gap junction channel subtypes. *Proc Natl Acad Sci U S A* **98**, 10942–10947.

Taccola G & Nistri A (2004). Low micromolar concentrations of 4-aminopyridine facilitate fictive locomotion expressed by the rat spinal cord in vitro. *Neuroscience* **126**, 511–520.

Taccola G & Nistri A (2005). Characteristics of the electrical oscillations evoked by 4-aminopyridine on dorsal root fibers and their relation to fictive locomotor patterns in the rat spinal cord in vitro. *Neuroscience* **132**, 1187–1197.

Todd AJ (1996). GABA and glycine in synaptic glomeruli of the rat spinal dorsal horn. *Eur J Neurosci* **8**, 2492–2498.

Tresch MC & Kiehn O (2000). Motor coordination without action potentials in the mammalian spinal cord. *Nat Neurosci* **3**, 593–599.

Varela F, Lachaux JP, Rodriguez E & Martinerie J (2001). The brainweb: phase synchronization and large-scale integration. *Nat Rev Neurosci* **2**, 229–239.

Whittington MA, Traub RD, Kopell N, Ermentrout B & Buhl EH (2000). Inhibition-based rhythms: experimental and mathematical observations on network dynamics. *Int J Psychophysiol* **38**, 315–336.

Yoshimura M & Jessell T (1990). Amino acid-mediated EPSPs at primary afferent synapses with substantia gelatinosa neurones in the rat spinal cord. *J Physiol* **430**, 315–335.

Author contributions

All of the authors have contributed to this study. Experiments were performed by P.C.L.C. and R.J.C. at the University of Leeds.

Acknowledgements

This work was supported by The Wellcome Trust, UK. P.F.C.L.C. held a BBSRC Committee studentship.

Author's present address

A. U. R. Asghar: Hull York Medical School & Department of Biological Sciences, University of Hull, Hull HU6 7RX, UK.